International Journal of Fluid Machinery and Systems
Vol. 2, No. 2, April-June 2009

Original Paper

Experimental Study on Internal Flow of a Mini Centrifugal Pump by PIV Measurement

Yulin Wu, Huijing Yuan, Jie Shao and Shuhong Liu

State Key Laboratory of Hydro Science and Hydraulic Engineering
Department of Thermal Engineering, Tsinghua University
Beijing, 10084, China

Abstract

The internal flow field in a centrifugal pump working at the several flow conditions has been measured by using the particle image velocimetry (PIV) technique with the laser induced fluorescence (LIF) particles and the refractive index matched (RIM) facilities. The impeller of the centrifugal pump has an outlet diameter in 100mm, and consists of six two-dimensional curvature backward swept blades of constant thickness. Measured results give reliable flow patterns in the pump. It is obvious that application of LIF particle and RIM are the key methods to obtain the right PIV measured results in pump internal flow

Keywords: Centrifugal pump, PIV, laser induced fluorescence, refractive index matched.

1. Introduction

Experimental flow studies are often conducted using optical diagnostic techniques including qualitative flow visualization methods, laser Doppler velocimetry (LDV), and more recently full field methods such as particle image velocimetry (PIV) for velocity field measurements, and laser induced fluorescence (LIF) for concentration field measurements. A difficulty common to all these methods is the refraction of light passing through gas-solid or liquid-solid interfaces of model and/or test section walls (Budwig, 1994) [1].

In the past, both computational fluid dynamics (CFD)[2,3]and experimental flow visualization have been performed to reveal flow characteristics in mini pumps and to examine a specific design. Li et al.[4] studied the interior viscous flow in a mini pump with an asymmetric axis using the PIV method. Pedersen et al.[5] investigated the flow inside the rotating channel of a six-bladed shrouded centrifugal pump impeller using PIV and LDV. Kadambi et al.[6] utilized PIV to investigate the velocities and kinetic energy fluctuations of slurry particles at the tongue region of an optically-clear centrifugal pump.

Performing PIV measurements within complex turbomachinery with multiple blades is difficult due to the optical obstruction to the illuminating sheet and to the camera caused by the blades. Uzol et al. (2001) has introduced a refractive index matched facility to overcome this problem[7]. The rotor and stating parts were made of transparent acrylic resin and the working fluid has the same optical refractive index as the rotor and parts. The refractive index of acrylic resin used in this work is 1.49 and a 64% by weight solution of Sodium Iodide in water is used for this purpose.

In this paper, the PIV measurement both with laser induced fluorescence (LIF) particle and refractive index matched (RIM) facilities in a centrifugal pump with 100mm diameter impeller have been carried out at several flow rates operating conditions.

The impeller under investigation is a centrifugal pump impeller as shown in Fig.1. It consists of six two-dimensioned curvature backward swept blades of constant thickness with arc profile leading edges and blunt trailing edges. The axial height of the impeller blade is tapered linearly from 15.13 mm at the inlet to 8.11 mm at the outlet. The entire impeller and the casing are all manufactured of acryl for the PIV measurements at impeller channels. Table 1 summarizes the main dimensions of the test impeller.

Received May 4 2009; accepted for publication May 5 2009: Review conducted by Prof. Yoshinobu Tsujimoto. (Paper number O09012)
Corresponding author: Yulin Wu, Professor, wyl-dhh@tsinghua.edu.cn

2. Experimental Apparatus

2.1 Centrifugal Impeller

The impeller under investigation is a centrifugal pump impeller as shown in Fig.1. It consists of six two-dimensioned curvature backward swept blades of constant thickness with arc profile leading edges and blunt trailing edges. The axial height of the impeller blade is tapered linearly from 15.13 mm at the inlet to 8.11 mm at the outlet. The entire impeller and the casing are all manufactured of acryl for the PIV measurements at impeller channels. Table 1 summarizes the main dimensions of the test impeller.

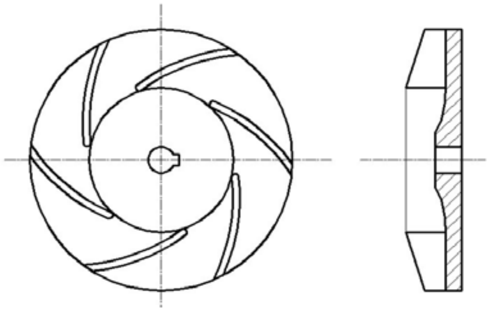

Fig. 1 Blade-to-blade and meridional view of the centrifugal impeller

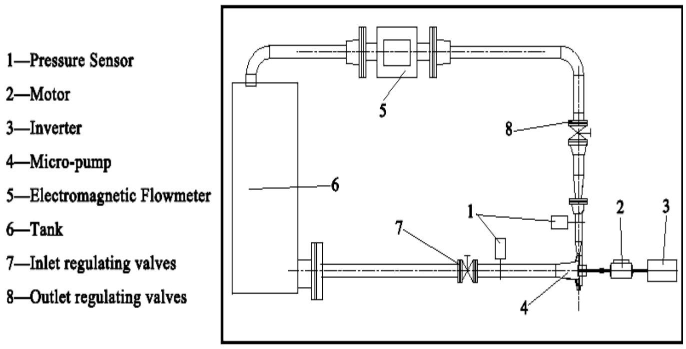

Fig. 2 The outline of the pump closed-loop

Table 1 Impeller geometry

Geometry	Symbol	Value	Unit
Inlet diameter	D_1	55.14	mm
Outlet diameter	D_2	100	mm
Inlet height	b_1	15.13	mm
Outlet height	b_2	8.11	mm
Number of blades	Z	6	–
Blade thickness	t	2.7	mm
Inlet blade angle	β_1	15	deg.
Outlet blade angle	β_2	39	deg.
Tip clearance	b	0.3	mm

2.2 The Experimental Set-Up.

Pump Loop Facility

An outline of the pump closed-loop is shown in Fig.2. The water flow rate is measured by an electromagnetic flow meter which is located downstream of the pump discharge and controlled by the inlet and out regulating valves. The angular speed is controlled by an inverter and fixed to 1000rpm for this study. The water head is measured by two pressure sensors.

The flow in the loop is delivered by an optically clear centrifugal pump. The PIV system is triggered as a function of impeller blade position by using an optical shaft encoder placed 5cm away from the shaft and aligned with one of the blades of the impeller.

The Optically Clear Centrifugal pump

The pump is specially designed to provide optical access. The casing and the impeller of the pump (Fig.3) are made from optically transparent acrylic resin. The ratio of pump casing inlet diameter to the discharge diameter is 1.5. The impeller has six blades.

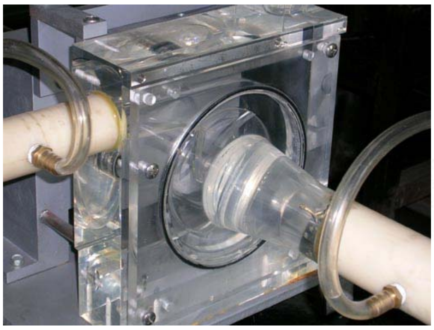

Fig. 3 Centrifugal pump with casing and impeller

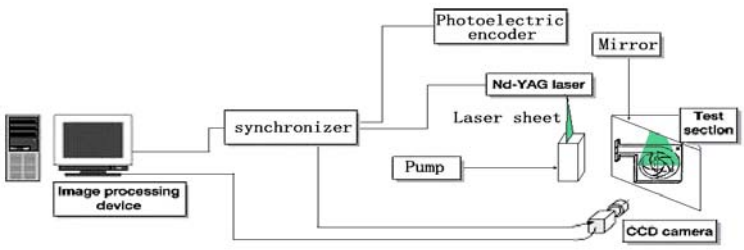

Fig. 4 The PIV setup

PIV System

PIV is a technique which measures the instantaneous velocity field within an illuminated plane of fluid field by using light scattered from particles seeded into the fluid [8] PIV has recently matured to a reliable technique that is used in a wide variety of applications[9] Fig. 4 shows the PIV setup. The PIV hardware for this research consists of a 120mJ/pulse dual-cavity pulsed Nd:YAG laser, laser light sheet optics, a charge coupled device (CCD) camera, a synchronizer and a dates process system.

In order to eliminate the effect of refraction/reflection light from the area close to the walls and enhance the measurement accuracy, fluorescent particles were scattered into the working fluid with the tracing particles. The refractive index of water in pump and of the transparent material of pump impeller and casing with curved walls is different. The beams of rays with different angles of incidence can not focus at a definite point, which will result in imaging defocused and deformed, and so in an error of PIV measurement. The RIM fluid with the same refractive index as the transparent material has been prepared and applied in the present test of pump with geometrical complex walls.

Figs. 5 (a) and (b) show the regions of interest in the casing and impeller of the centrifugal pump. Because the space behind the pump is too small for installing the CCD camera, a mirror settled with 45° angle was used. Measurements could be performed through the mirror in the facility specially designed to provide an unobstructed view of the flow. The examined plane is located at the middle of the blade outlet height.

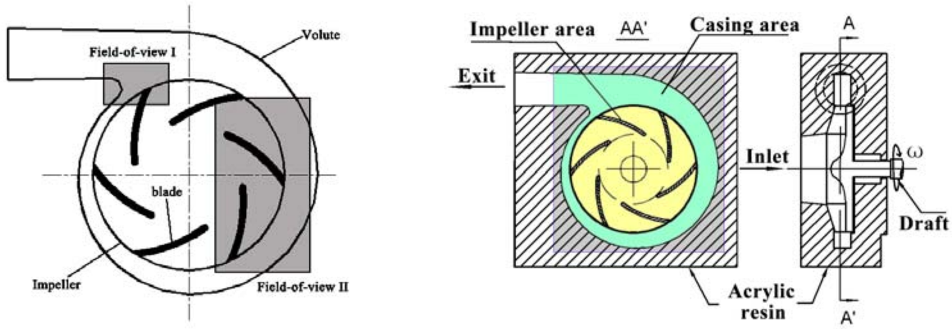

(a) (b)

Fig. 5 Locations of measured file in the pump

Pairs of single exposured image frames were required for cross-correlation date processing. The image pairs are processed by TSI Insight software. The image pairs acquisition were synchronized with the impeller rotation by using a optical trigger which located at the pump shaft

3. Results and discussion

3.1 Hydrodynamic performance of the pump

The hydrodynamic performances of the centrifugal pump are shown in Fig. 6. The performances are expressed as the pump-generated water head versus flow rate curve (*H-Q* curve) and the pump efficiency versus flow rate curve (η–Q curve) at the specific rotation speed (1000rpm). The CFD simulation by DES simulation was performed at 7 operating conditions. The flow rate of the operating conditions is 30%~1.30% of the designed flow rate. The computationally predicted water head at these conditions is in very good agreement with the experimentally measured water head.

3.2 The internal flow of the mini centrifugal pump

Comparison between results with and without RIM

In order to get velocity distribution in pump, one hundred image frame pairs are acquired for each operating condition. Cross-correlation processing is used to get the ensemble averaged velocity vector maps for particle flow. Fig. 7 shows PIV measurement results of absolute velocity (a) with and (b) without the refractive index matched (RIM) facility in impeller. Fig. 7 (a) illustrates the clear velocity distribution on the complex flow area, such as, between impeller blade and tongue, but in (b), the velocity distribution is not fine. The prepared RIM fluid is used as the circulation liquid in the test loop. The refractive index of this mixture nearly equals to that of acryl material to get clear and non distorted digital images and the true flow velocity distribution in complex area in water flow field is obtained.

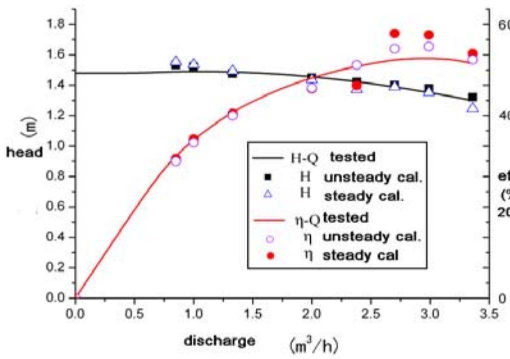

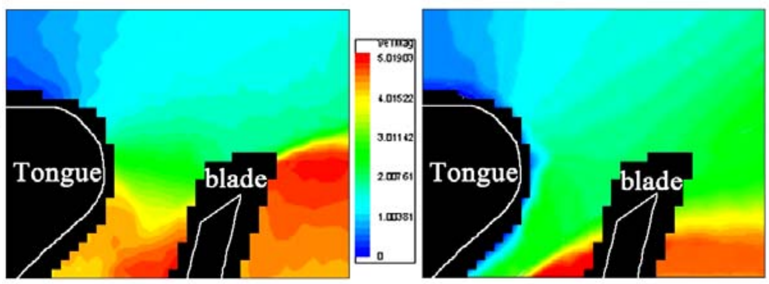

(a) with RIM (b) without RIM

Fig. 6 The performance curve of pump

Fig. 7 Comparison of test results with and without RIM

Comparison between results with and without LIF

From Fig. 8, one may find that with laser induced fluorescent seeds of PIV image near walls can be obtained. Without fluorescent seeds the laser will be reflected from walls, the clear images near walls will be destroyed by the highlight laser beam, In some cases, the sensor plate of CCD camera may be destroyed.

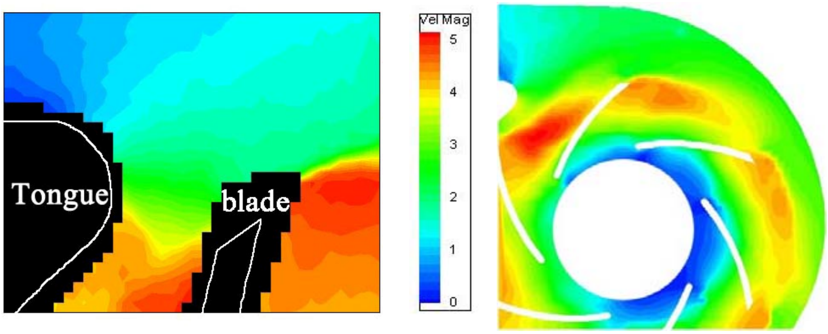

(a) without LIF and with RIM (b) with LIF and RIM

Fig. 8 Comparison of results with and without LIF and RIM

Comparison between results of test with LIF and RIM and simulation

Fig. 9 indicates the comparison between test results with LIF / RIM and the simulated by using DES. Thevelocity distributions at investigation area obtained by PIV and calculated by DES showed a satisfactory agreement at the design operation condition, with flow discharge 2.70 m^3/s and head 1.40 m.

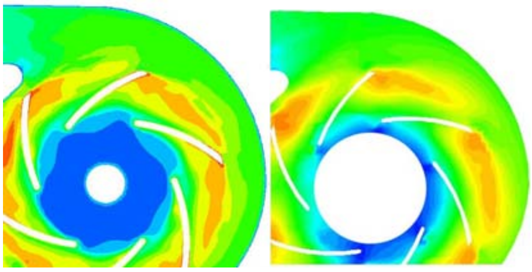

(a) DES simulation (b) Test data

Fig. 9 Internal flow velocity (m/s) in the pump of simulated and experimental results

Relative velocity distribution and streamlines in impeller at design condition

Fig.10 shows the relative velocity and streamlines distribution in impeller at design discharge condition (Q=Q_d= 2.70m^3/s). In Fig. 10, there are 5 pictures (a) to (e) to display the velocity for different position of impeller vanes. The time interval between two positions is one fifth of period T of impeller rotation. The flow distributions on 5 pictures are almost the same, that illustrates the impeller manufactured axisymmetrically and also the measurement with reliability. The flow difference in different blade channels occurs near the tongue, which affects the flow in the channel greatly.

At the design condition, the relative velocity in the blade channel distributes smoothly and decreases from inlet to exit. And at impeller exit, the relative velocity is lower close to suction side than that near pressure side of blade in most of blade channels. This flow structure is somewhat of jet-wake flow structure in centrifugal impeller. This is because the blade exit angle is 40^o and is greater than that of conventional centrifugal pump. There are some differences in flow patterns between different blade channels. The relative velocity in the blade channel close to pump exit is higher than that in other channels. The relative streamlines in blade channel distribute along the blade surface and there is not any circulation in the channel at the rated condition. Fig. 11 shows the absolute velocity and streamlines in casing at design discharge condition. The flow distributions on 5 pictures of casing are almost the same, and they are smooth and almost even. Near the tongue the absolute velocity is higher than that in other position.

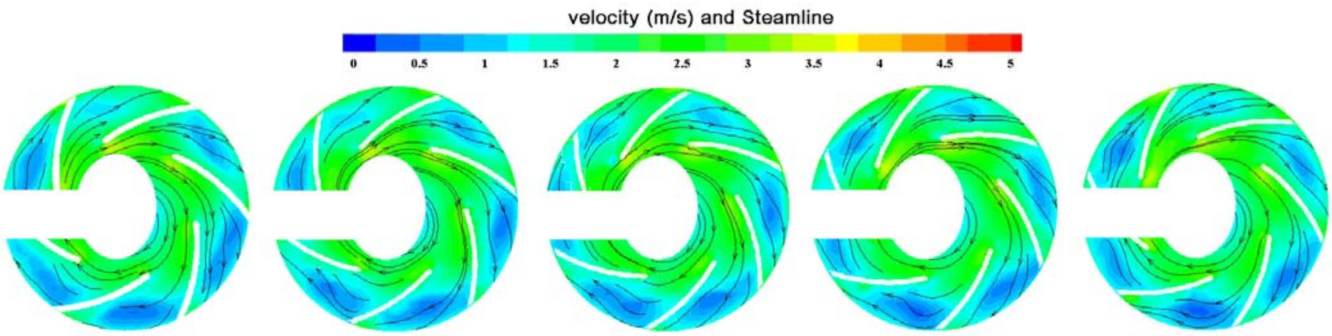

(a) t=0 (b) t=T/5 (c) t =2T/30 (d) t =3T/5 (e) t =4T/5

Fig. 10 Relative velocity and streamlines in impeller at design discharge condition（Q=Q_d）

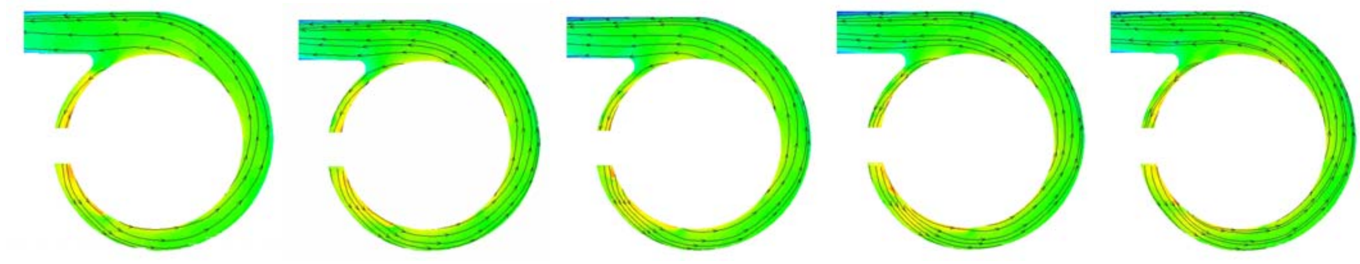

(a) t=0 (b) t=T/5 (c) t =2T/30 (d) t =3T/5 (e) t =4T/55

Fig. 11 The absolute velocity and streamlines in casing at design discharge condition (Q=Q_d)

Relative velocity distribution and streamlines in impeller at small discharge condition

Fig.12 and Fig. 13 show the relative velocity and streamlines distribution in impeller and the absolute velocity and streamlines in casing, respectively, at small discharge condition (Q=52%Q_d= 1.404m^3/s)

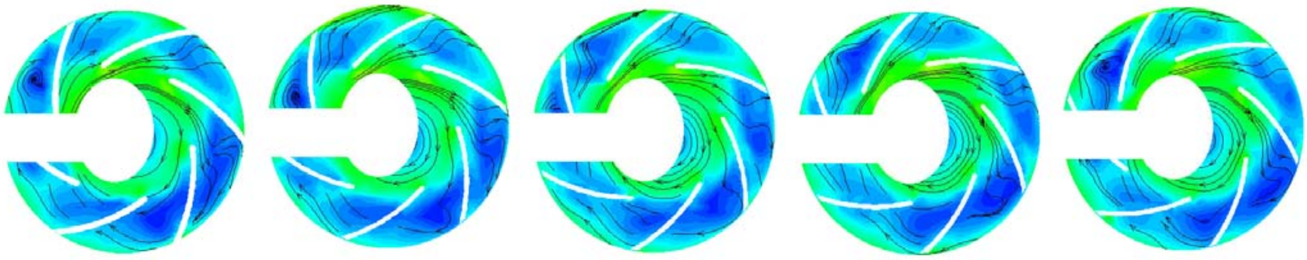

(a) t=0 (b) t=T/5 (c) t =2T/30 (d) t =3T/5 (e) t =4T/5

Fig. 12 Relative velocity and streamlines in impeller at small discharge condition (Q=52%Q_d)

From Fig. 12, it is clear that the low relative velocity area appears at the impeller exit near blade suction surfaces. And the relative velocity in the blade channel close to the casing tongue is rather larger at blade exit than that in other blade channels. The relative velocity direction in those channels is not along the tangent direction of the blade surface caused by inlet positive attack angle at blade entrance and by the flow separation near suction surfaces at the small discharge condition. One may note that the relative velocity distributions at different time moments are not the same and that a circulation area appears at one blade channel near casing tongue and is fixed at the position while the impeller rotates. This is the fixed stalling in the impeller.

From Fig. 13, it is clear that the velocity at casing exit is low, and the low velocity area appears at the upper position near the exit. The velocity distribution and streamlines in the casing vary with impeller rotation, but those variations are very small.

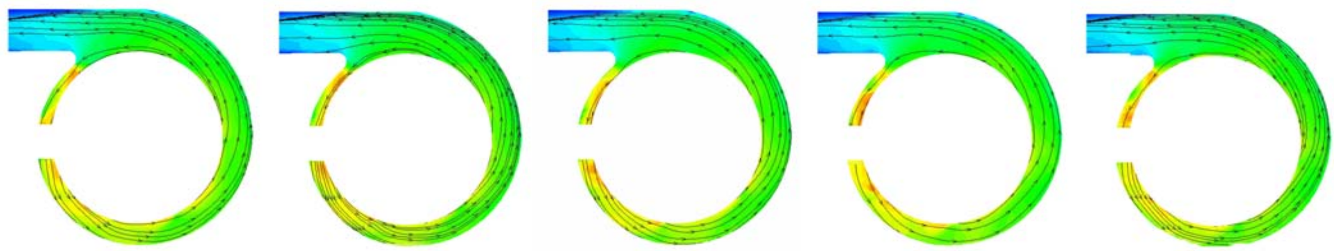

(a) t=0 (b) t=T/5 (c) t =2T/30 (d) t =3T/5 (e) t =4T/5

Fig. 13 The absolute velocity and streamlines in casing at small discharge condition (Q=52%Q_d)

Relative velocity distribution and streamlines in impeller at large discharge condition

Fig. 14 shows the relative velocity and streamlines distribution in impeller and Fig. 15 the absolute velocity and streamlines in casing, respectively, at large discharge condition (Q=124%Q_d= 3.348 m^3/s).

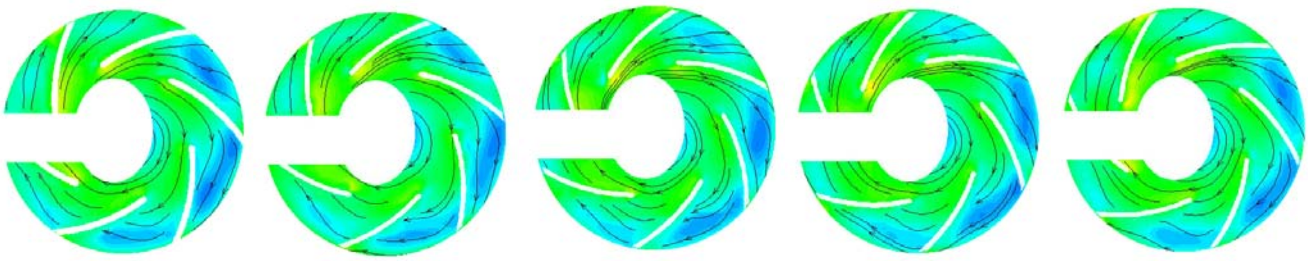

(a) t=0 (b) t=T/5 (c) t =2T/30 (d) t =3T/5 (e) t =4T/5

Fig. 14 Relative velocity and streamlines in impeller at large discharge condition (Q=124%Q_d)

In Fig. 14, it is shown that the low relative velocity area appears at the impeller exit near blade suction surfaces, it is the same situation at the design case. And the relative velocity in the blade channel close to the casing tongue is rather larger at blade exit than that in other blade channels. The relative velocity direction in those channels is basically along the tangent direction of the blade surface. One may note that the relative velocity distributions at different time moments are not the same, but that a circulation area is not found at one blade channel near casing tongue.

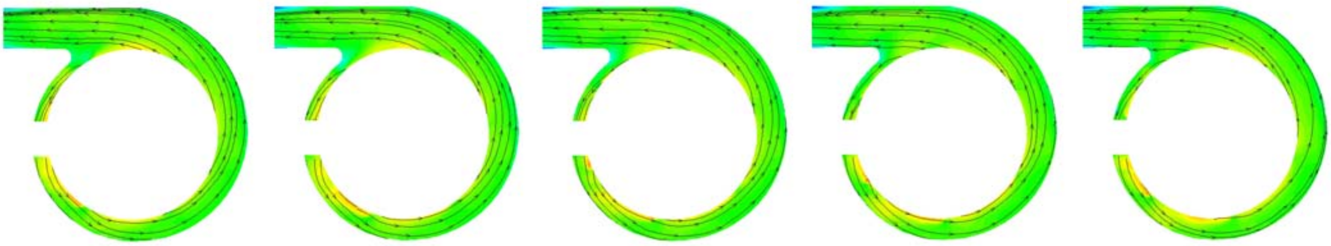

(a) t=0 (b) t=T/5 (c) t =2T/30 (d) t =3T/5 (e) t =4T/5

Fig. 15 The absolute velocity and streamlines in casing at large discharge condition (Q=124%Q_d)

In Fig. 15, it is shown that the velocity in the casing is the largest at the large discharge condition among those at three cases measured. The flow direction is almost the same as that at design case. The flow pattern seems to be fixed in blade channels as impeller rotating.

4. Conclusions

(1) The water head and efficiency of the centrifugal pump at different operation conditions agree very well with computational prediction by DES simulation.
(2) The present PIV measurement both with the laser induced fluorescence (LIF) particles and the refractive index matched (RIM) facilities in a centrifugal pump with 100mm diameter impeller has been carried out at the three flow rate operating conditions and gives a reliable flow patterns in the pump. It is obvious that the application of LIF particle and RIM are the key methods to get good PIV measurement results in pump internal flow.
(3) PIV measurements show that flow distributions on 5 pictures at different times are almost same, and illustrate the impeller manufactured axisymmetrically and also the measurements with reliability at design discharge condition.
(4) At the design condition, the relative velocity in the blade channel distributes smoothly and decreases from inlet to exit. And at the impeller exit, the relative velocity is lower close to suction side than that near pressure side of blade in most of blade channels. The flow patterns at large and small discharge conditions are also identified.
(5) At the low discharge condition, the relative velocity distributions at different time moments are not the same and that a circulation area appears at one blade channel near casing tongue and is fixed at the position while the impeller rotates.

Acknowledgments

This work has been supported by the National Natural Science Foundation of China (No. 10532010).

References

[1] Budwig, R., 1994, Refractive index matching methods for liquid flow investigations, Experiments in Fluids 17 (1994) 350-355.
[2] Burgreen, G.W. and Antaki, J.F., 1996, CFD-based design optimization of a three-dimensional rotary blood pump, American Institute of Aeronautics and Astronautics (AIAA) Paper 96-4185, Proc 6th Symp on Multidisciplinary Analysis and Optimization, Bellevue, WA, pp. 1773-1778.
[3] Burgreen, G.W., Antaki, J.F. and Butler, K.C., 1998, CFD-based design optimization of the outlet stator of a rotodynamic cardiac assist device. American Institute of Aeronautics and Astronautics (AIAA) Paper 98-4808, Proc 7th Symp on Multidisciplinary Analysis and Optimization, St Louis, MO, pp. 818-824.
[4] Li, J.W., Liu, S.H., Luo, X.W. and Wu, Y.L., 2007, Viscous flow field in a small pump. *J. of Tsinghua Univ. (Sci&Tech)*, Vol. 47, No.5, pp. 682-685.
[5] Pedersen, N, et al., 2003, Flow in a Centrifugal Pump Impeller at Design and off-design conditions−Part I: Particle Image Velocimetry (PIV) and Laser Doppler Velocimetry (LDV) Measurements. Journal of Fluids Eng., Vol. 125, pp. 61-72.
[6] Kadambi, J. R., et al., 2004, Investigations of Particle Velocities in a Slurry Pump Using PIV: Part 1, The Tongue and Adjacent Channel Flow, Journal of Energy Resources Technology. Vol. 126, pp: 271-278.
[7] Uzol, U., Chow, Y.C., Katz, J. and Meneveau, C., 2001, Unobstructed PIV measurements within an axial turbo-pump using liquid and blades with matched refractive indices, 4th International Symposium on Particle Image Velocimetry Göttingen, Germany, September 17-19, 2001 PIV'01 Paper 1085.
[8] Adrian, R. J., 1991, "Particle Imaging Techniques for Fluid Mechanics," Annu.Rev. Fluid Mech. 23, pp. 261-304.
[9] Keane, R. D., and Adrian, R. J., 1992, "Theory of Cross-Correlation Analysis of PIV Images," Appl. Sci. Res. 49, pp. 191-215.